

Numerical validation of aerodynamics for two in-line model wind turbines using actuator line model and CFD technique

Yong Ai, Ping Cheng, Decheng Wan*

Collaborative Innovation Center for Advanced Ship and Deep-Sea Exploration, State Key Laboratory of Ocean Engineering, School of Naval Architecture, Ocean and Civil Engineering, Shanghai Jiao Tong University, Shanghai, China

*Corresponding author: dcwan@sjtu.edu.cn

ABSTRACT

In this present study, a numerical validation of aerodynamics for two in-line model wind turbines using actuator line model and CFD technique. The actuator line model is used to simulate the blades of two in-line model wind turbines while the hub, nacelle and tower of both two wind turbines are not included in present study. The SST $k-\omega$ turbulence model is applied to solve the RANS equation due to the closure problem. The uniform free-stream flow condition at a speed of 10 m/s at the reference height of hub is applied to the inlet. Upstream and downstream wind turbines are running at tip speed ratio 6 and 4 respectively. The result from the present simulation is compared to the experiment data. From the comparison, the results from the present study show a good agreement with the experimental results especially for the aerodynamic loads prediction taking the aerodynamic power and thrust into account yielding a maximum error of 3% for the upstream wind turbine and maximum error of 10% for the downstream wind turbine. Another conclusion can be easily drawn that although difference in wake prediction exists in the simulation for two in-line wind turbines model comparing to the blind test2, the actuator line model still can yield the distribution characteristics of the mean wake velocity and mean turbulent stress. Such as the number and position of peaks, the wake width is also can be captured with acceptable accuracy.

Keywords: aerodynamic loads, wake prediction, actuator line model, blind test 2.

1 INTRODUCTION

Wind energy is a promising renewable energy resource to help handle the environmental pollution caused by the extended use of fossil fuel. Wind farm, which has large capacity to contain plenty of wind turbines, is becoming the main mode in the utilization of wind energy. The aerodynamics plays a significant role in the wind farm. How to simulate the wind farm accurately and efficiently is becoming an important task especially in the study of aerodynamics.

In order to study the complex phenomenon existing in wind farms, lots of wake models depending on some assumptions were developed. For example, Katic et al.^[2] proposed a one-dimension wake model called Park wake model and applied it to the wind resource evaluating software. Pierella et al.^[3] pointed out in his study that most of the early models relied heavily on assumptions and shortcuts which needed to be calibrated against experimental data. With development in experimental technology, the experimental technique is becoming more and more advanced. However, it is unrealistic to use the experimental method to study the wake interaction for wind farms in full scale because of the high cost and the long-time period. Vermeer et al.^[4] pointed out that in totally full scale experiments used for comparison, the inflow conditions are usually not well defined and may contain a fair amount of uncertainty, and the limited amount of data available often makes a comparison difficult. More recently, full scale and model scale CFD techniques have been employed in order to resolve the flow much more in detail. Two options are basically available: either fully resolving the blade geometry with its boundary layers or modelling the rotor as a force field. From the work of Zahle et al.^[5] and work from Choi et al.^{[6][7]}, it can be concluded that the full wind turbine model

wind farm simulation is computationally demanding. The actuator line model created by Sørensen et al [8] is a very useful and popular approach to model the rotor as a force field. Some researchers have finished lots of work for the wind farm simulation using actuator line model. A high-fidelity tool SOWFA [9] (*Simulator for Wind Farm Applications*), which is a LES framework coupled with FAST [10] (*Fatigue, Aerodynamics, Structures, Turbulence*), was used to analyse offshore wind turbine and wind farm based on that method. Troldborg and Larsen [11] presented numerical simulations of wake interaction between two wind turbines in various inflow condition using actuator method coupled with EllipSys3D [12] software. Churchfield, Lee and Moriarty [13] have done a large-eddy simulation of the 48 multi-megawatt turbines composing the Lillgrund wind plant. Fleming et al [14]. presented a Simulation comparison of wake mitigation control strategies for a two-turbine case. Although there are lots of work to simulate the wind farm to study the aerodynamics and wake interaction, a full validation of the accuracy against the experiment is still needed, only that can we do more meaningful studies about the wind farm to research the aerodynamics and significant wake interaction.

In this present study, a numerical validation of aerodynamics for two in-line model wind turbines using actuator line model and CFD technique is conducted and compared to blind test 2 to validate the aerodynamic loads prediction including the aerodynamic power and aerodynamic thrust and wake prediction including the Mean Velocity Profile Mean turbulent stress profile at X=1D, 2.5D and 4D at downstream of the downstream wind turbine. Furthermore, the vortex structure in a full rotating period is also presented in this study.

2 NUMERICAL METHODS

2.1 Actuator line model

The actuator line model (ALM) was firstly developed by Sørensen and Shen (2002). The rotating blades are virtualized into span wise sections of constant airfoil, chord and twist with certain load distribution including the drag and lift forces. Hence, there is not requirement to build the actual blades model. Moreover, the lift force and drag force of each section can be calculated as:

$$L = \frac{1}{2} C_l(\alpha) \rho U_{rel}^2 c dr \quad (1)$$

$$D = \frac{1}{2} C_d(\alpha) \rho U_{rel}^2 c dr \quad (2)$$

Where, C_l and C_d are the lift and drag coefficient, respectively. α is the attack angle, c is the chord length, U is the local velocity relative to the rotating blade of each section.

The local velocity as shown in figure 1 between the flow and the rotating blades is given by

$$U_{rel} = \sqrt{U_z^2 + (\Omega r - U_\theta)^2} \quad (3)$$

Where Ω is the rotational speed of the turbine and r is the radius of the blade. The angle between the relative velocity U_{rel} and the rotor plane is

$$\varphi = \tan^{-1} \left(\frac{U_z}{\Omega r - U_\theta} \right) \quad (4)$$

The local angle of attack is defined by

$$\alpha = \varphi - \gamma \quad (5)$$

Where γ is the local collective pitch angle.

f denoted body force is calculated per spanwise length corresponding to the chord length of the blade and the local velocity, it can be expressed as

$$f = (L, D) = \frac{1}{2} \rho U_{rel}^2 c \left(C_l \vec{e}_L + C_d \vec{e}_D \right) \quad (6)$$

Where \vec{e}_L and \vec{e}_D are the unit vector in the direction of the lift and drag forces respectively and c represents the chord length. The lift and drag coefficients used to calculate the force are given as tabulated airfoil data.

The applied aerodynamic blade forces need to be distributed smoothly on several mesh points in order to avoid singular behaviour. In practice, a 3D Gaussian function is chosen to smooth the force over every blade by taking the convolution of the force with a regularization kernel, where

$$\eta_\varepsilon(d) = \frac{1}{\varepsilon^2 \pi^{3/2}} \exp\left[-\left(\frac{d}{\varepsilon}\right)^2\right] \quad (7)$$

Here, d is the distance between cell-centred grid points and the actuator line point, and ε is parameter that serves to adjust the concentration of the regularized loads.

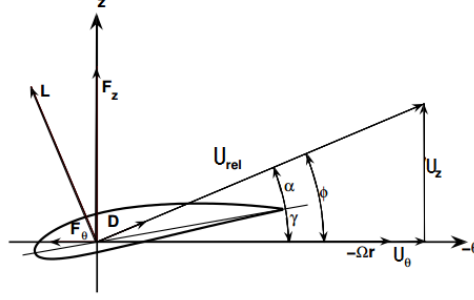


Figure 1: Cross-sectional aero foil element^[7]

2.2 Governing Equation

In the present study, the RANS equation was solved, the expression can be written as:

$$\frac{\partial U}{\partial x_i} = 0 \quad (8)$$

$$\frac{\partial U_i}{\partial t} + \frac{\partial}{\partial x_j} (U_i U_j) = -\frac{1}{\rho} \frac{\partial p}{\partial x_i} + \frac{\partial}{\partial x_j} \left(\nu \frac{\partial U_i}{\partial x_j} - \overline{u'_i u'_j} \right) + \frac{1}{\rho} f \quad (9)$$

Where U is the velocity of flow; ρ is the density of the fluid; p is the pressure; ν is the kinematic viscosity and f denotes the body force, which represents the loading on the rotating blades. The body force acting on the blades is determined by a blade element method combined with tabulated two-dimensional airfoil characteristics. The SST k - ω turbulence model is applied to solved the RANS equation due to the closure problem, in which the turbulent kinetic energy k and the turbulent dissipation rate can be expressed as:

$$\frac{\partial}{\partial t} (\rho k) + \frac{\partial}{\partial x_i} (\rho k u_i) = \frac{\partial}{\partial x_j} \left(\Gamma_k \frac{\partial k}{\partial x_j} \right) + G_k - Y_k + S_k \quad (10)$$

$$\frac{\partial}{\partial t} (\rho \omega) + \frac{\partial}{\partial x_i} (\rho \omega u_i) = \frac{\partial}{\partial x_j} \left(\Gamma_\omega \frac{\partial \omega}{\partial x_j} \right) + G_\omega - Y_\omega + D_\omega + S_\omega \quad (11)$$

Where, Γ_k and Γ_ω are the effective diffusion coefficients for the turbulent kinetic energy k and the turbulent dissipation rate ω respectively, G_k and G_ω are turbulence generation terms, Y_k and Y_ω are turbulent dissipation terms, D_ω is the cross-diffusion term for ω , S_k and S_ω are the source term.

3 SIMULATION SETUP

3.1 Introduction to blind Test 2

The Blind test 2 was organized by Norcowe and Nowitech in Trondheim, Norway in October 2012. This experiment carried out in the large close-loop wind tunnel facility at NTNU was arranged to figure out how well wind turbine simulation models perform when it is applied to two turbines operating in line. The wind tunnel has a rectangle test section, whose dimensions at the inlet are $W=2.72$ m and $H=1.80$ m (W means width and H means height). The test section is $L_{1/4}=11.15$ m long, and the roof height was adjusted in order to produce zero pressure gradient in the whole test section at the reference velocity used in the tests when the tunnel was empty. The reference velocity was set to $U_{ref}=10$ m/s. At this velocity, the turbulence intensity was $TI=0.3\%$ at the inlet. More detail about the blind test 2 can be found in reference [16].



Figure 2: wind tunnel

3.2 Wind turbine model

Like the blind test 2, there are also two same wind turbines in an in-line layout in the present study. The two wind turbines have the same blade geometry, but slightly different hub size, leading to different rotor diameter. The diameter of upstream and downstream wind turbine is 0.944 m and 0.894 m, respectively. Table 1 gives some specification of the two wind turbines used in this present study.

Table 1: parameters of two wind turbines

Items	WT1	WT2
Airfoil	S826	S826
Rotor Diameter	0.944 m	12-point
Nacelle Diameter	0.13 m	0.09 m
Height of tower	0.817 m	0.817 m
Pitch Angle	0	0
Tip Speed Ratio	0	4

3.3 Case description

In order to compare to blind test 2, the computation of the numerical study is stayed as the same dimensions with the wind tunnel in NTNU mentioned above. The whole length along the flow direction is 11.15 m, the width and height is 2.72 m and 1.8 m respectively. The upstream wind turbine is positioned at 2D from the test section inlet. It was verified that this location is sufficiently far downstream for the operation of the turbines not to affect the uniformity of the inlet velocity profile. The downstream turbine T2 is positioned at 3D downstream from the upstream turbine, and both turbines had the same hub height 0.817 m, so the distance between the centre of two wind turbine rotor plane and ground is kept the same as the hub height 0.817 m.

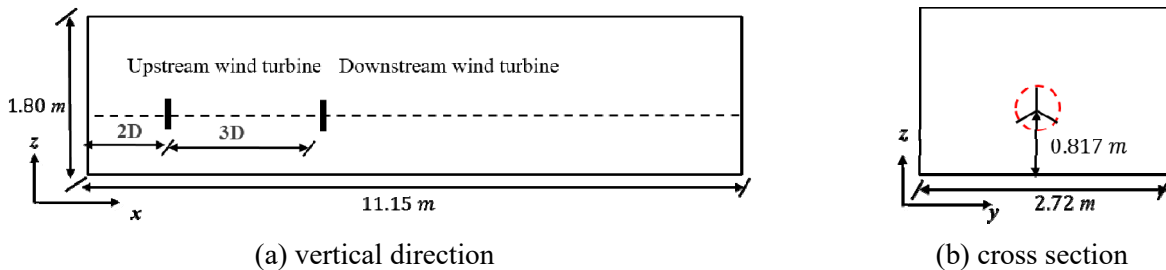


Figure 3: computation setup, dimension

The mesh system for the whole numerical computation contains four parts to fully resolve the strong gradients in the vicinity of the actuator lines. The first part generated by the OpenFOAM mesh tool BlockMesh is an initial mesh part for the whole flow field. Considering the computational time, there are three refinements based on the initial mesh part. The range of first refinement whose level is one is from -0.5 D to 8D in the flow direction and from -1.25D to 1.25 D in width direction and from the bottom to 2 D in height direction. In this present study, the D is the diameter of downstream wind turbine. The range of

second refinement with secondary level is from $-0.25 D$ to $7.5D$ in the flow direction and from $-D$ to D in width direction, the range of height direction is from $0.25D$ to $1.75D$. In order to capture the tip vortex, it is necessary to conduct the third mesh refinement. The range of third refinement in three levels is from $-0.5 D$ to $8D$ in the flow direction and from $-1.25D$ to $1.25 D$ in width direction and from the bottom to $2 D$ in height direction. Finally, the total mesh was controlled about 11.56 million for the numerical case.

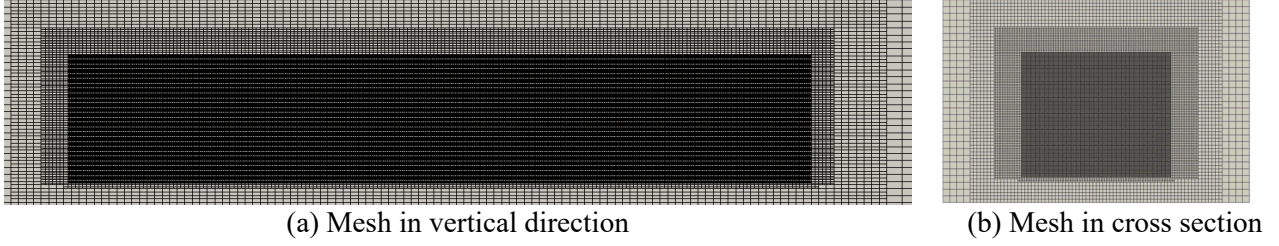


Figure 4: The grid in lengthwise section and cross section

The reference velocity of at the hub height in this experiment is 10 m/s and with low turbulent uniform free-stream flow. Thus, the numerical study of the two in-line model wind turbines is set to be the same reference velocity at the speed of 10 m/s. The airfoil data of blades calculated by the XFOIL^[15] is prepared to be the interpolation database, which contains the lift and drag coefficient, and the twist angle of each section in different blade sections. The tip speed ratios of upstream and downstream win turbine are 6 and 4 respectively.

In this study, the uniform free-stream flow condition at the speed of 10m/s is applied to the inlet defined in Figure 2, respectively. A relative pressure of 0 Pa based on the atmospheric pressure is chosen for outlet boundary. Free-slip condition is applied to the top boundary, which means there is no wind speed gradient vertically and no flow across the top surface. Considering the bottom boundary as the sea surface, the no slip condition is applied to it and the sidewall 1 and sidewall 2 boundary are set to symmetry.

To ensure that the flow is fully developed in most of the wake, the computation duration is about 2.34 seconds. The computational time step is given to $1.3e-4s$ considering the CFX condition to avoid the numerical divergence. In addition, more accurate numerical data could be obtained in this study. Meanwhile, the parameter ϵ existed in Eq. 7 and named Gaussian width parameter, has a significant influence in the CFD simulation. This value of ϵ is roughly the minimum at which the force is smoothed enough to avoid spurious oscillations in the resulting velocity field using a central spatial discretization scheme^[11]. In this study, according to some conclusions drawn by other researchers, the parameter ϵ is kept to be equal to twice the local grid size around the blades.

4 RESULTS AND DISCUSSIONS,

In this present study, a numerical validation of aerodynamics for two in-line model wind turbines using actuator line model and CFD technique is conducted and compared to blind test 2 to validate the aerodynamic loads prediction including the aerodynamic power and aerodynamic thrust and wake prediction including the Mean Velocity Profile Mean turbulent stress profile at $X=1D$, $2.5D$ and $4D$ at downstream of the downstream wind turbine. Furthermore, the vortex structure in a full rotating period is also presented in this study.

4.1 Aerodynamic loads prediction

The time history curves of aerodynamic loads are showed in figure 5. Figure 5 (a) shows the time-history of aerodynamic power while figure 5 (b) is the time-history of aerodynamic thrust. The upstream wind turbine operates at tip speed ratio 6 and the downstream wind turbine runs at lower tip speed ratio 4. The numerical and experimental value from the blind test 2 are summarized in table 2. The power coefficient and thrust coefficient in table 2 are defined as

$$C_p = \frac{2P}{\rho U_{ref}^3 A} \quad (12)$$

$$C_T = \frac{2T}{\rho U_{ref}^2 A} \quad (13)$$

Where A is the rotor disk area using the actual rotor diameters, $D1$ and $D2$. ρ is air density and U_{ref} is reference velocity at the hub center. P and T are the aerodynamic power and aerodynamic thrust, respectively.

From the table 2, it can be figured out that the aerodynamic power coefficient of upstream wind turbine resulted from the numerical simulation based on actuator line model is about 0.481 while the experimental value from the blind test 2 is about 0.469. Compared to experimental results, the actuator line model overestimated the power coefficient for the upstream wind turbine but the relative error of 2.559% is in a reasonable range. The similar phenomenon occurred in the aerodynamic thrust coefficient. The thrust coefficient calculated by the actuator line model is about 0.867 and the thrust coefficient from the blind test 2 is about 0.883. it can be concluded that the actuator line model for the aerodynamic thrust prediction, which gives an offset from the experimental value of only about 1.8% performed quite well. From the validation of aerodynamic loads against the results from blind test 2, it can be concluded that a prediction with promising accuracy of aerodynamic load including the aerodynamic power and thrust for the upstream wind turbine when simulation for two in-line wind turbines by using the actuator line model and CFD technique to model the wind turbine blade. There is reasonable error for the engineering application. We can also figure out the aerodynamic power prediction for the downstream wind turbine has little different with the upstream wind turbine. The power coefficient of the downstream wind turbine is about 0.129 while power coefficient from the experiment is about 0.121, thus there is a little large relative error compared with the upstream wind turbine, there is about 6.6% offset from the blind test 2. The aerodynamic thrust coefficient is computed to be $C_T=0.392$ by the actuator line model in the numerical simulation while measured to be $C_T=0.363$ in the blind test 2. The relative error of aerodynamic thrust for the downstream wind turbine reaches to be about 8%.

Table 2: summary of numerical results for aerodynamic power coefficient and aerodynamic thrust coefficient and the results for blind test 2. Where WT1 represents the upstream wind turbine and WT2 is the downstream wind turbine

Items		Present study	Experiment	Relative error
C_P	WT1	0.481	0.469	2.559%
	WT2	0.129	0.121	6.608%
C_T	WT1	0.867	0.883	1.812%
	WT2	0.392	0.363	8.098%

Compared with the aerodynamic loads coefficient of upstream wind turbine, there is a much larger relative error of the aerodynamic loads for the downstream wind turbine neither the aerodynamic power nor aerodynamic thrust prediction based on the actuator line mode using the CFD technique. After analysis for the case, it indicates that there are some main reasons causing the relative error for the aerodynamic loads prediction. First, when the upstream and downstream wind turbines operate at the tip speed ratio 6 and 4 respectively, the two turbines may operate in a sensitive Reynolds number flow condition which has a significant influence on the airfoil data especially the lift and drag coefficient. When the reference velocity is 10m/s, the tip local Reynolds number is about 10^5 for the upstream turbine at maximum performance. On the other hand, the tip local Reynolds number is lower for the downstream wind turbine due to the lower tip speed ratio and experiencing lower velocity flow. Thus, there is a totally different Reynolds number compared to the upstream wind turbine. But the airfoil data tabulated for interpolation with respect to the Reynolds number is only suitable for the upstream in theory not for the downstream wind turbine. In the numerical simulation, there is only one airfoil database tabulated for both two wind turbines in the actuator line model to calculate body force. There is Little offset of aerodynamic loads including the power and thrust for the upstream wind turbine from the experimental results, whereas there is higher relative error of aerodynamic loads for the downstream wind turbine. Second, owing to lacking of the fully wind turbine model including the blades, hub, nacelle and tower which may also have a great influence in the flow and speed deficit, nevertheless, the actuator line model uses a force field to simulate the rotor and cannot consider the hub, nacelle and tower in present study, the flow field may have somewhat different compared to the flow field considering the fully resolved wind turbine system. Thus, due to the strong wake interaction, there may be quite complex wake around the downstream wind turbine. There is quite big challenge for actuator line model to simulate the whole flow accurately. The last reason for the relative error may be that the blockage efforts of the wind tunnel. In the actual wind tunnel experiment, there is an unavoidable effort

named blockage which is not easy to consider correctly in numerical simulation. In present simulation, the left and right boundary is regarded as symmetry plane rather than the wall boundary, which may be one of the most significant reasons to cause much larger error compared to blind test 2.

From the discussion above, it can be concluded that the numerical simulation for two in-line wind turbine model shows a good agreement for the aerodynamic load prediction, both of the power and thrust. Although there is error especially for the downstream wind turbine. It can be figure out that there may be some reasonable reasons exiting. The difference of Reynolds number for the upstream and downstream wind turbines may lead to big difference of aerodynamic performance. Furthermore, the lack of real model and the blockage effects may also have significant influence on it. However, the totally highest error is not over 10%, it is quite enough to the engineering application.

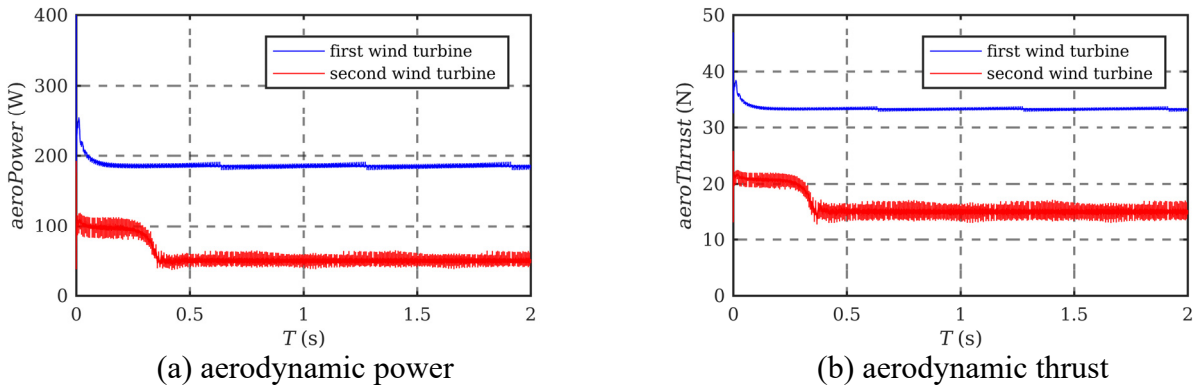


Figure 5: time-history curves of aerodynamic Load. the left figure is the aerodynamic power while the right is the aerodynamic thrust.

4.2 Wake prediction

Figure 6-8 show the wake prediction including the mean wake velocity and mean turbulent stress at three positions ($X=1D$, $2.5D$, $4D$) behind the downstream wind turbine along the width direction while upstream and downstream wind turbines are running at tip speed ratio 6 and 4 respectively. The hub, nacelle and tower are not included in present simulation due to the ignorance the influence by hub, nacelle and tower of the present actuator line model.

At the one diameter position behind the downstream wind turbine wake, conclusions can be drawn that the mean wake velocity profile calculated from the simulation using actuator line model coupled into the OpenFOAM tool is more symmetrical in shape compared to the experimental results marked in filled circles in figure 6 (a) which is slightly asymmetric. The difference may cause by the tower which will have a quite significant influence on the wake. The wake generated by the tower is mixed with the wake produced by the rotor, which will lead to a quite complex wake velocity profile in the blind test 2 considering the influence of tower while the present simulation ignores the tower effects in the actuator line model. Moreover, velocity outside the wake computed by the actuator line model is only 10% higher than the reference velocity while the velocity measured in experiment outside of the wake is 20% higher than the reference velocity. Similar results are also captured in the position $X=2.5D$ and $X=4D$. The outside of wake is close to the left and right boundary which may cause big blockage effects of wind turbine. In present study, there is no consideration of the blockage effects of wind turbine due to the boundary condition of the left and right boundary which is set to symmetry condition rather than the wall condition while the wind tunnel experiment can include the effects. This is the main reason why the velocity outside of wake is lower than the value from the experiment, which may have other influence on the whole flow field. thus, causing big error discussed in above chapter for the aerodynamic loads. Another main difference between the simulation and experiment is the velocity of the wake centreline. The simulation conducted by Acona and CMR marked with dark yellow square in figure 6-8(a), which includes the blades, hub, nacelle and tower, shows a good agreement with the experiment especially for the velocity of wake centreline while the simulation conducted by ElliSys3D which does not include the blades, hub, nacelle and tower presents a similar result to the present study. From the comparison, the main reason is that no including the hub and nacelle causes the big difference in the velocity of wake centreline in this present study.

Although there are some differences in the mean wake velocity profile, there is still some good agreement against the blind test 2. The wake width is similar to the results from the experiment. Small error is presented in the velocity profile computed by actuator line model at $Y=\pm R$ position against the experimental result. Furthermore, two low peaks appear roughly at $Y=\pm R$ position in the experiment at the position $X=1D$ behind the downstream wind turbine wake region. The similar phenomenon is also captured by present study and one higher peak around the wake centreline is also watched in this simulation, which is also similar to the experimental results.

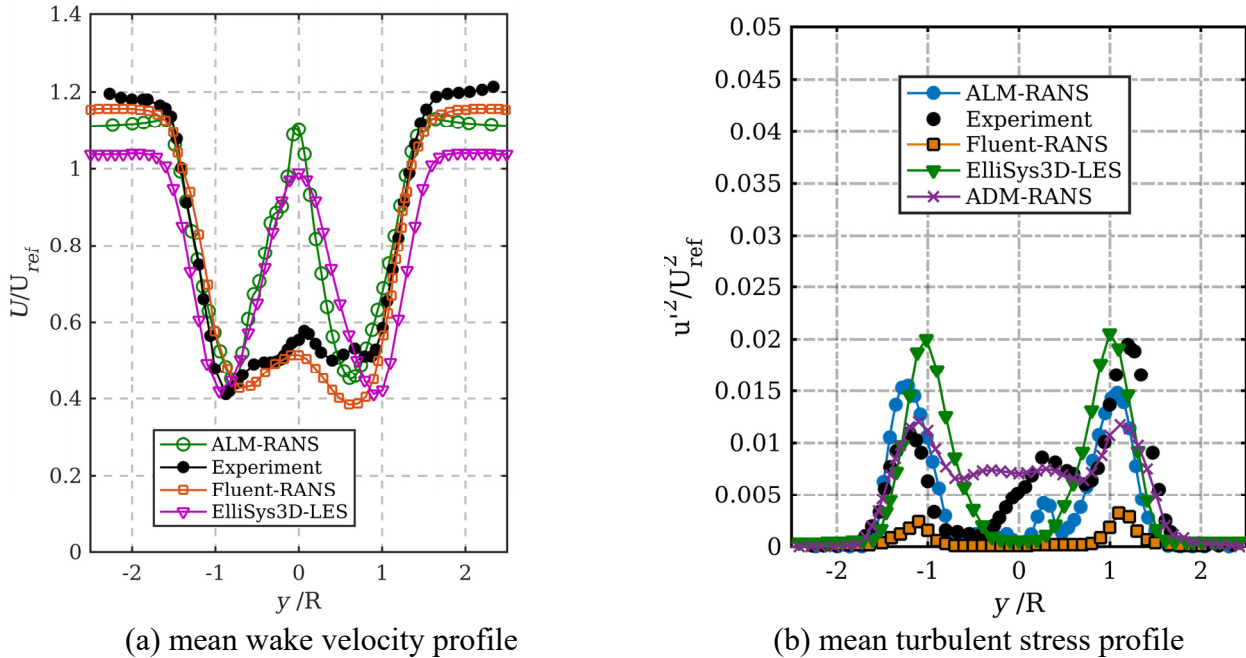


Figure 6: wake prediction for mean wake velocity and mean turbulent stress at one diameter position behind the downstream wind turbine along the width direction while upstream and downstream wind turbines are running at tip speed ratio 6 and 4 respectively. The hub, nacelle and tower are not included in present simulation

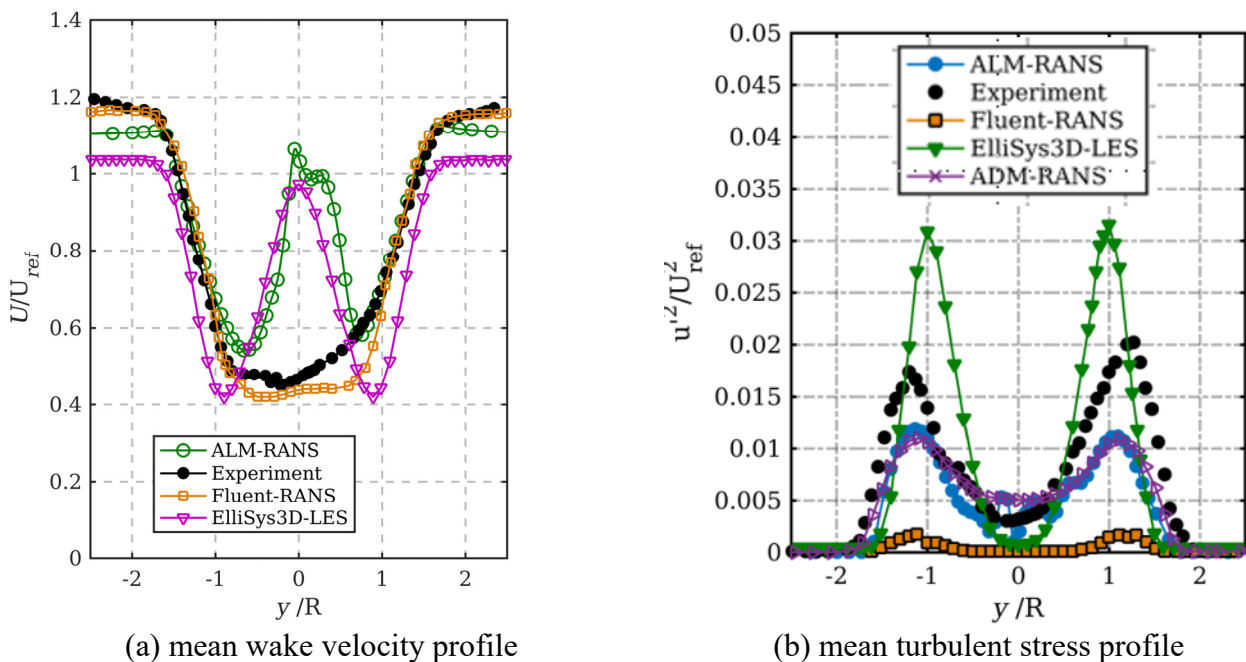


Figure 7: wake prediction for mean wake velocity and mean turbulent stress at two and a half diameters position behind the downstream wind turbine along the width direction while upstream and downstream

wind turbines are running at tip speed ratio 6 and 4 respectively. The hub, nacelle and tower are not included in present simulation

At $X=2.5D$ (figure 7(a)) behind the wake of downstream wind turbine, the velocity profile from present simulation is still symmetrical in shape and the present study still featured a high velocity peak at the wake centreline, while the velocity profile was wider and smoother than at the previous station, but still rather asymmetric. Similar result is also captured in the position $X=4D$ (figure 8(a)). The reason has been analysed in discussion above.

Two high peaks are captured in the Figure 6(b), the mean turbulent stress profile, similar phenomenon also occurs in figure 7(b) and figure 8(b). A small peak around the centreline exits at $X=1D$ (figure 6(b)). There is a good agreement with the experiment although the value of peaks is different. Comparison of mean turbulent stress between the position $X=1D$, $2.5D$ and $4D$, it shows that the present study underestimates the turbulent stress magnitude especially in the peaks, whose value is much lower than the blind test2. The similar conclusions can be also drawn from the results for ADM and Fluent. On the other hand, the result from the Ellisis3D shows a good agreement with the experimental value at position $X=1D$ and is higher than the experiment. It can be found that the results from the present study, ADM and Fluent both use the same turbulent model named RANS model. And the RANS models that use 2-equation turbulence closure approximations generally underestimated the turbulent stress magnitude and overestimated its dissipation rate, probably due to the anisotropy of the turbulent stresses.

From discussion above, it can be easily concluded that although the simulation for two in-line wind turbines model exit some big difference in wake prediction compared to the blind test 2, the actuator line model still can result in the distribution characteristics of the mean wake velocity and mean turbulent stress. Such as the number and position of peaks, the wake width is also can be captured roughly accurate. Furthermore, the aerodynamic loads prediction is still in a reasonable result.

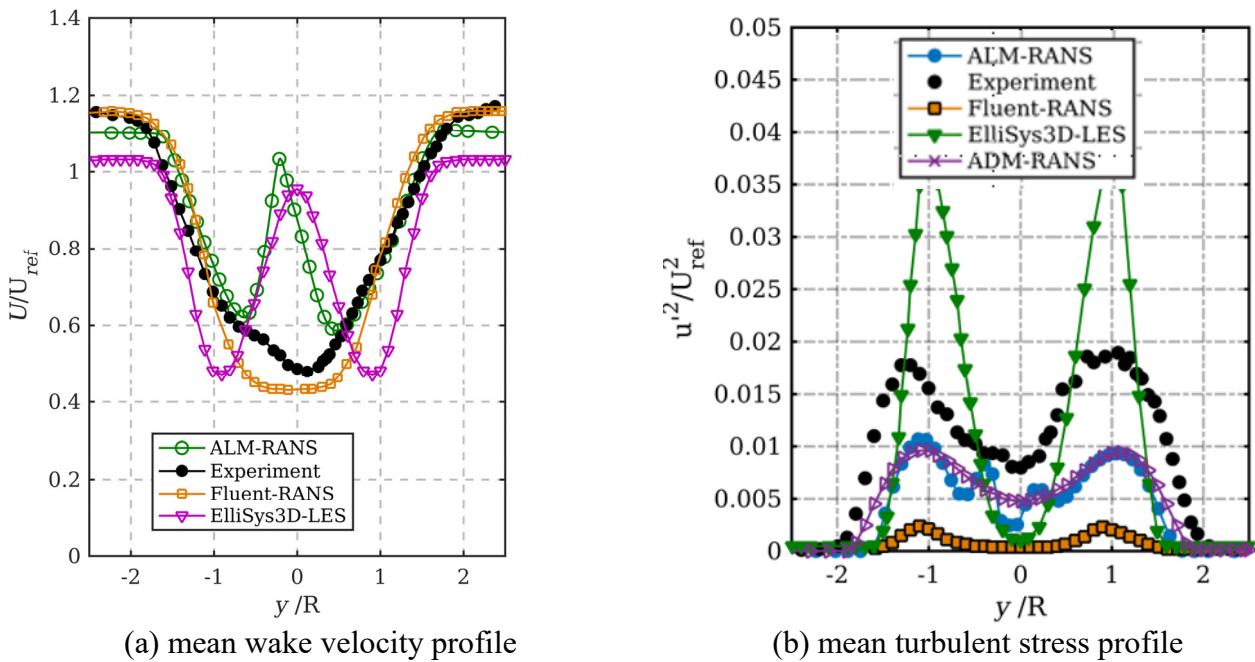


Figure 8: wake prediction for mean wake velocity and mean turbulent stress at four diameters position behind the downstream wind turbine along the width direction while upstream and downstream wind turbines are running at tip speed ratio 6 and 4 respectively. The hub, nacelle and tower are not included in present simulation

4.3 Vortex structure

Figure 9 shows the vortex structure in a full rotating period while the upstream and downstream wind turbines operate at tip speed ratio 6 and 4 respectively. it can be easily seen that there is clear tip vortex of the upstream wind turbine after fully developing of the flow field. With the development vortex, the distance of each blade vortex is becoming larger and larger. Furthermore, the vortex generated by upstream wind turbine is mixed with the vortex produced by downstream wind turbine, a series of grouped vortex is shaped as the development of the flow field. And the radius is larger than the initial vortex of upstream wind turbine due to

the wake expanding effects and the mixed vortex effects. From the development of the vortex for the two in-line model wind turbines, it can clearly figure out that there is obvious and strong wake interaction phenomenon exists in the two wind turbines wind farm, the wake interaction has great influence on power output, the speed deficit in the wind farm. it can be pointed out that there is big speed deficit in the inside of vortex, which may have significant influence on the downstream wind turbine especially to the aerodynamic power output.

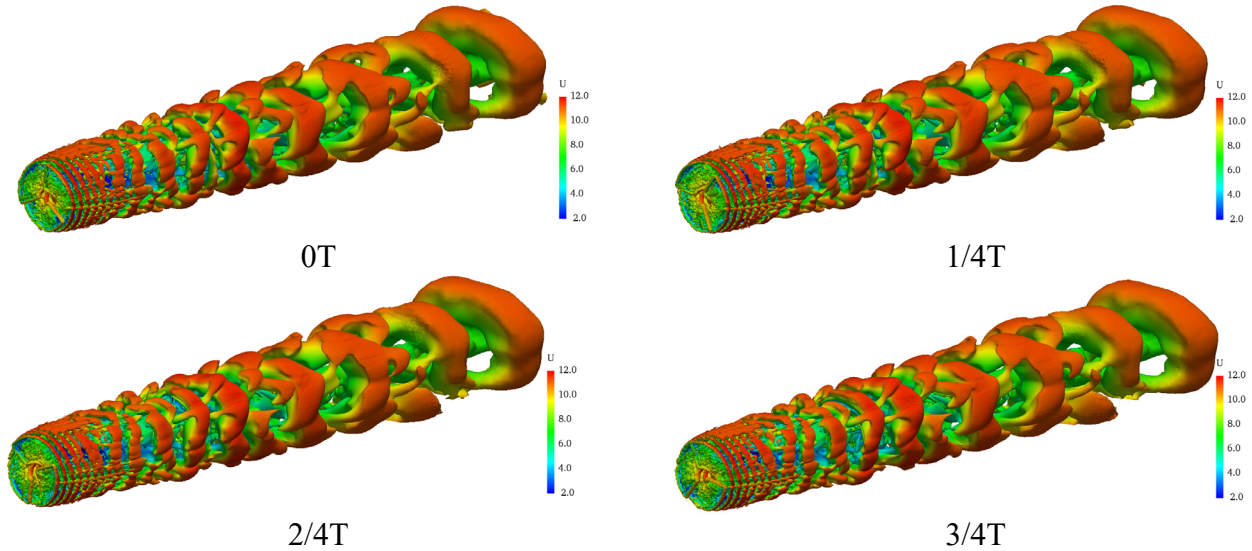


Figure 9: the vortex structure in a full rotating period while the upstream and downstream wind turbines operate at tip speed ratio 6 and 4 respectively

5 CONCLUSION

In this present study, a numerical validation of aerodynamics for two in-line model wind turbines using actuator line model and CFD technique. The actuator line model is used to model the blades of two in-line model wind turbines while the hub, nacelle and tower are not included in present study. The SST $k-\omega$ turbulence model is applied to solved the RANS equation due to the closure problem. The uniform free-stream flow condition at a speed of 10 m/s at the reference height of hub is applied to the inlet. Upstream and downstream wind turbines are running at tip speed ratio 6 and 4 respectively. The result from the present simulation is compared to the experiment data. From the comparison, the result from the present study shows a good agreement with the experimental results especially for the aerodynamic loads prediction taking the aerodynamic power and thrust into account yielding a maximum error of 3% for the upstream wind turbine and maximum error of 10% for the downstream wind turbine. The reason for the error is caused by three major reason. The lift and drag coefficient for the airfoil S826 in different Reynold number plays a key role in the simulation when the rotor was model with the force field. Moreover, owing to lack of the fully wind turbine model including the blades, hub, nacelle and tower which may also have a great influence in the flow and speed deficit. The blockage effects also have a significant influence to aerodynamics. Thus, it is necessary to consider the blockage effect to get more accurate results. However, the totally highest error is not over 10%, it is quite enough to the engineering application.

Another conclusion can be easily drawn that the simulation for two in-line wind turbines model exit some big difference in wake prediction compared to the blind test 2 due to no considering the influence of hub nacelle and tower, thus, there are some big difference in the mean wake velocity profile. From the comparison of different numerical simulations and experiment, it can be concluded that the RANS models that use 2-equation turbulence closure approximations generally underestimated the turbulent stress magnitude and overestimated its dissipation rate, probably due to the anisotropy of the turbulent stresses. Although there is some difference compared to the experiment, the actuator line model still can result in clearly the distribution characteristics of the mean wake velocity and mean turbulent stress. Such as the number and position of peaks, the wake width is also can be captured roughly accurate.

In the future work, the blockage effects could be included to do more accurate simulation, Furthermore, the LES simulation can be also used to study the wake interaction effects exiting in the wind farms to find more valuable information.

ACKNOWLEDGEMENTS

This work is supported by the National Natural Science Foundation of China (51379125, 51490675, 11432009, 51579145), Chang Jiang Scholars Program (T2014099), Shanghai Excellent Academic Leaders Program (17XD1402300), Shanghai Key Laboratory of Marine Engineering (K2015-11), Program for Professor of Special Appointment (Eastern Scholar) at Shanghai Institutions of Higher Learning (2013022), Innovative Special Project of Numerical Tank of Ministry of Industry and Information Technology of China(2016-23/09) and Lloyd's Register Foundation for doctoral student, to which the authors are most grateful.

REFERENCES

1. Ainslie, J. F. (1988). Calculating the flowfield in the wake of wind turbines. *Journal of Wind Engineering and Industrial Aerodynamics*, 27(1), 213-224.
2. Katic, I., Højstrup, J. and Jensen, N. O. (1987). A Simple Model for Cluster Efficiency. In W. Palz, & E. Sesto (Eds.), *EWEC'86. Proceedings*. Vol. 1 (pp. 407-410). Rome: A. Raguzzi.
3. Pierella, F., Krogstad, P. and Sætran, L. (2014). Blind Test 2 calculations for two in-line model wind turbines where the downstream turbine operates at various rotational speeds. *Renewable Energy*, 62-77.
4. Vermeer, L., Sorensen, J., and Crespo, A. (2003). Wind turbine wake aerodynamics. *Progress in Aerospace Sciences*, 39(6), 467-510.
5. Zahle, F., Sorensen, N. N. and Johansen, J. (2009). Wind turbine rotor-tower interaction using an incompressible overset grid method. *Wind Energy*, 12(6), 594-619.
6. Choi, N. J., Nam, S. H., Jeong, J. H. and Kim, K. C. (2013). Numerical study on the horizontal axis turbines arrangement in a wind farm: Effect of separation distance on the turbine aerodynamic power output. *Journal of Wind Engineering and Industrial Aerodynamics*, 117, 11-17.
7. Choi, N. J., Nam, S. H., Jeong, J. H. and Kim, K. C. (2014). CFD Study on Aerodynamic Power Output Changes with Inter-Turbine Spacing Variation for a 6 MW Offshore Wind Farm. *Energies*, 7(11), 7483-7498.
8. Sørensen, J. N. and Shen, W. Z. (2002). Numerical modeling of wind turbine wakes. *Journal of fluids engineering*, 124(2), 393-399.
9. Churchfield, M. and Lee, S. NWTC design codes (SOWFA), 2013.
10. Jonkman, J. (2010). NWTC design codes (FAST). <https://nwtc.nrel.gov/FAST>.
11. Troldborg, N., Larsen, G. C., Madsen, H. A., Hansen, K. S., Sørensen, J. N. and Mikkelsen, R. (2011). Numerical simulations of wake interaction between two wind turbines at various inflow conditions. *Wind Energy*, 14(7), 859-876.
12. Michelsen, J. A. (1994). Block structured Multigrid solution of 2D and 3D elliptic PDE's. Department of Fluid Mechanics, Technical University of Denmark.
13. Churchfield, M. J., Lee, S., Moriarty, P. J., Martinez, L. A., Leonardi, S., Vijayakumar, G. and Brasseur, J. G. (2012). A large-eddy simulation of wind-plant aerodynamics. *AIAA paper*, 537, 2012.
14. Fleming, P., Gebraad, P. M., Lee, S., Van Wingerden, J., Johnson, K. E., Churchfield, M. J., ... and Moriarty, P. (2015). Simulation comparison of wake mitigation control strategies for a two-turbine case. *Wind Energy*, 18(12), 2135-2143.
15. Drela M. (1989). XFOIL: An Analysis and Design System for Low Reynolds Number Airfoils. Technical Report, NREL. DOI: 10.1007/978-3-642-84010-4_1
16. Pierella, F., Eriksen, P. E., Sætran, L. and Krogstad, P. Å. (2012). Invitation to the 2012" Blind test 2" Workshop Calculations for two wind turbines in line. Dept. Energy and Process Eng., NTNU, Trondheim, Norway.
17. Krogstad, P. Å. and Eriksen, P. E. (2013). "Blind test" calculations of the performance and wake development for a model wind turbine. *Renewable energy*, 50, 325-333.
18. Li, P., Cheng, P. and Wan, DC (2015). Numerical Simulation of Wake Flows of Floating Wind Turbines by Unsteady Actuator Line Model[C]. *Proceedings of the 9th International Workshop on Ship and Marine Hydrodynamics (IWSH2015)*, Glasgow, UK.
19. Li, P., Wan, DC. and Hu, H. Fully Coupled Dynamic Response of a Semi-submerged Floating Wind Turbine System in Wind and Waves, *Proceedings of the Twenty-sixth (2016) International Ocean and Polar Engineering Conference Rhodes*, Greece, June 26-July 1, 2016, 273-281
20. Zhao, W., Cheng, P., Wan, DC. (2014). Numerical Computation of Aerodynamic Performances of NREL Offshore 5-MW Baseline Wind Turbine[C]. *The Proceedings of the Eleventh (2014) Pacific/Asia Offshore Mechanics Symposium (PACOMS-2014)*, Shanghai, China, October 12-16, 2014, ISOPE, 13-18.
21. Ai, Y., Wan, DC. and Hu, C. (2017). Effects of Inter-Turbines Spacing on Aerodynamics for Wind Farms Based on Actuator Line Model[C]. *Proceedings of the Twenty-seven (2017) International Ocean and Polar Engineering Conference*, San Francisco, California, USA, June 25-30, 2017, ISOPE, pp. 386-394.

22. Huang, Y., Wan, DC and Hu, C. (2017). Coupled Aero-hydrodynamic Analysis on a Floating Offshore Wind Turbine under Extreme Sea Conditions[C]. *Proceedings of the Twenty-seven (2017) International Ocean and Polar Engineering Conference*, San Francisco, California, USA, June 25-30, 2017, ISOPE, pp. 395-402.
23. Cheng, P. and Wan, DC. (2017). Analysis of wind turbine blade-tower interaction using overset grid method, *Chinese Journal of Hydrodynamics*, Vol. 32, No. 1, pp. 32-39.